ABNUS JOURNAL
Your Research Partner

Jurnal Teknika dan Informatika (JTI)
E-ISSN: 2797-0000 | Vol. 1, No. 2 (2021) | pp. 80–103

Simulation Analysis of Fuel Injection Performance in Four-Stroke Gasoline Engine Intake Manifold Systems

Rasyid Hadi Sudono[1*]

[1] *Faculty of Engineering and Informatics, a Mechanical Engineering Study Program, Dian Nusantara University, Jakarta, Indonesia*

***Corresponding author:** rasyid.sudono@undira.ac.id |

Received: 20 September 2021 | Revised: 21 October 2021 | Published: 30 November 2021

Abstract

Purpose: This study aims to analyze the characteristics of fuel injection in the intake manifold of a four-stroke gasoline engine using numerical modeling and simulation methods.
Research Methodology: The study was conducted by modeling an injector using mathematical equations and varying the inlet speed.
Results: The simulation results revealed that as the inlet speed increased, the fluid injection points shifted faster. The wall area exhibited low speed due to the boundary layer effect, indicating poor fuel and air mixing in those areas.
Conclusions: The study demonstrates that varying inlet velocities significantly affect the speed and pressure distribution patterns within the intake manifold. Higher inlet velocities cause the spray point to shift more rapidly, enhancing fuel-air mixing in specific areas. The velocity vector distribution revealed vortex patterns around the spray points, further contributing to the mixing process.
Limitations: This study is limited by the specific conditions in the ANSYS FLUENT simulations, such as constant temperature and pressure, which may not represent real-world variations. Moreover, only a single injector model was examined, and future research could explore multiple injector configurations and their impacts under different operational conditions.
Contributions: This research enhances the understanding of how inlet velocity influences fuel-air mixing in gasoline engines. By using ANSYS FLUENT, the study offers valuable insights into velocity, pressure, and flow patterns in the intake manifold. These findings have implications for optimizing fuel injection systems in four-stroke gasoline engines, contributing to improved engine performance and efficiency.

Keywords: *ANSYS Software, Computational Fluid Dynamics, Injector, Speed Flow*

How to Cite: Sudono, R. H. (2021). Simulation Analysis of Fuel Injection Performance in Four-Stroke Gasoline Engine Intake Manifold Systems. *Jurnal Teknika dan Informatika (JTI)*, *1*(2), 80–103.
https://doi.org/10.52909/jti.v1i1.12

1. Introduction

A piston engine is a type of combustion engine that converts chemical energy into thermal energy, which is then converted into mechanical energy (Ayuningtyas & Ilman, 2021; Rao et al., 2018). A piston engine is an internal combustion engine (ICE). There are three types of piston engines: gasoline, gas (OTT), and diesel. The difference between these three types is that an Otto engine uses gasoline and gas, whereas a diesel engine uses diesel fuel (Aljaberi et al., 2017; Wahyuningsih et al., 2021). The main

difference between the two is the ignition system. Gasoline engines use spark plugs, whereas diesel engines utilize high compression temperatures to ignite diesel fuel (Ikeya et al., 2015). A gasoline engine is a piston engine. In a gasoline engine, the fuel is ignited by an electric spark generated between two iron electrodes. Fuel mixing occurs outside the cylinder (i.e., combustion chamber) (Dinh et al., 2020; Kalita & Titabor, 2016; Syahrial & Sudono, 2021). In a conventional gasoline engine, fuel and air are mixed using a carburetor(Anakottapary, 2020; Berlian Rms & Wahyuningsih, 2021).

To achieve optimal performance from a gasoline engine, the fuel and air must be mixed perfectly to meet the engine's needs (Saputro & Soleha, 2021). Therefore, technological developments in this mixing process have been undertaken, and the carburetor has been replaced with a fuel injection system. The goal of this development is to improve the performance of previous technologies, including addressing the engine's need for a more balanced fuel-air mixture (Benajes et al., 2017; Ricardianto et al., 2021). Furthermore, this technology meets the demands for more economical fuel consumption and increased engine performance. In gasoline engines, fuel injection is expected to achieve complete combustion of the fuel (Susanto et al., 2021). Therefore, the fuel must be properly mixed with air before entering the combustion chamber. The fuel injection system has sensors that can respond to the fuel needs of the engine. This thesis discusses the characteristics of the fuel spray in the intake manifold using numerical modeling simulation methods for a four-stroke gasoline engine (Chala et al., 2018; Kalghatgi & Johansson, 2018; Parmenas, 2021).

In order to effectively model the fuel injection process, it is essential to understand how different variables, such as injector design, fuel pressure, and inlet velocity, influence the atomization and mixing of the fuel-air mixture (Barot et al., 2017; Setyawati et al., 2021). The study utilizes Computational Fluid Dynamics (CFD) simulations to simulate the flow of fuel and air through the intake manifold of a four-stroke gasoline engine (Galamboš et al., 2020; Mishra et al., 2016; Susanto & Parmenas, 2021). By using advanced CFD software such as ANSYS FLUENT, this research aims to analyze how varying inlet velocities affect the fuel injection process and the subsequent combustion efficiency (Holkar et al., 2015; Inam et al., 2019; Xu & Choa, 2016). Additionally, the study will explore how the geometry of the intake manifold and injector nozzle configuration impact the dispersion and uniformity of the fuel-air mixture (Jumadi et al., 2020; Setyawati & Aristiyanto, 2021). The results from this simulation will provide valuable insights into the optimization of fuel injection systems, contributing to improved engine performance, fuel efficiency, and reduced emissions. Ultimately, this work seeks to enhance the understanding of the fluid dynamics involved in fuel injection and assist in the design of more efficient internal combustion engines.

2. Literature Review

2.1 Motor Burn

A combustion engine is a machine or device that uses thermal energy to perform mechanical work by converting the chemical energy of the fuel into heat energy and using this energy to perform mechanical work (Heriyanto, 2021; Kuncoro & Harahap, 2021). Thermal energy is obtained from the combustion of fuel in an engine (Agusinta et al., 2021; Anggraini, 2021). When viewed from the method of obtaining thermal energy (the fuel combustion process), combustion engines can be divided into two groups: external and internal combustion engines (Descombes et al., 2003; Kunze & Stimming, 2009). In this external combustion process, the fuel combustion process occurs outside the engine; therefore, a separate engine is used to carry out the combustion (Keke et al., 2021). The heat from combustion is first transferred through a conducting medium and then converted into mechanical energy. For example, a boiler or steam turbine (Saputro & Soleha, 2021). Internal combustion engines: In internal combustion engines, fuel combustion occurs within the engine, converting the heat generated directly into mechanical

energy. For example, gas turbines and reciprocating engines (Aprillita & Perkasa, 2021; Wallington et al., 2006).

2.2 Principle Work Motor Gas

This energy is then used to generate a mechanical motion. The working principle of a gasoline engine can be explained as follows: a mixture of air and fuel from the carburetor is drawn into the cylinder. It is then compressed. by the piston moment move go on. When the mixture of air and material burns with the existence of a spark from the spark plug, it produces high combustion gas pressure inside the cylinder (Abdullah, 2021; Abu-Qudais et al., 2001). This combustion gas pressure pushes the piston down, which moves the piston freely up and down inside the cylinder, as shown in Figure 1. The linear (upward and downward) motion of the piston is converted into rotary motion on the crankshaft via the piston rod. This rotary motion generates power for vehicles.

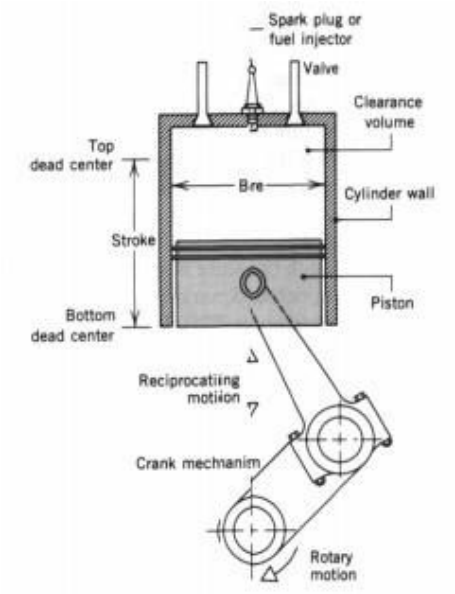

Figure 1. Torak and Mechanism Cranking

Based on Figure 1, the highest position reached by the piston in the cylinder is called the top dead center (TDC), and the lowest position reached by the piston is called the bottom dead center (BDC). The distance the piston moves between the BDC and TDC is called the piston stroke. The air and fuel mixture is sucked into the cylinder and the burned gas must be released, and this must occur continuously (Andwari et al., 2018; Goyal et al., 2019). This work is performed by the piston moving up and down in the cylinder. The process of sucking the air and fuel mixture into the cylinder, compressing it, burning it, and expelling the used gas from the cylinder is called a cycle. Additionally, there is an engine in which each cycle consists of two piston strokes. This engine is called a 2-stroke engine (two-stroke engine). The crankshaft rotates once, whereas the piston completes two strokes. In other engines, each cycle consists of four strokes of the piston (Satria, 2021; Solihin, 2021). This engine is called a four-stroke engine. The crankshaft rotates two complete revolutions, whereas the piston completes four strokes in each cycle.

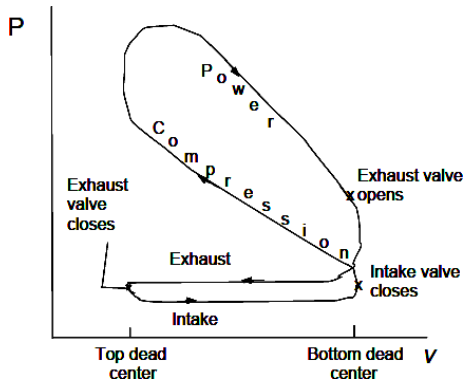

Figure 2. Cycle Machine

Figure 2 shows the pressure-volume (P-V) cycle of a four-stroke engine, illustrating the stages of compression, power, exhaust, and intake. It depicts the movement of the piston from top dead center (TDC) to bottom dead center (BDC), with valve actions for each phase.

2.3 Principle Work Machine 4 Step

The principle of the Work motor gas is explained in Figure 3 as follows:

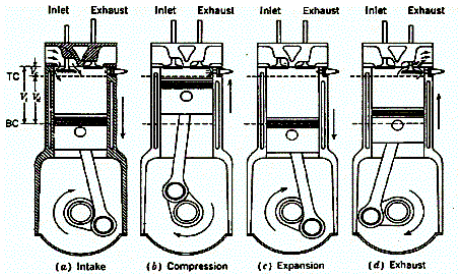

Figure 3. Principle Work Machine 4 Step

Based on Figure 3, the piston reciprocated up and down inside the cylinder. The highest point reached by the piston is called the top dead center (TDC), and the lowest point is called the bottom dead center (BDC). The movement from the TDC to the BDC is called the piston stroke. In a 4-stroke engine, there are four steps in one movement: the intake, compression, power, and exhaust strokes (Aljaberi et al., 2018; Nassiri et al., 2017).

1. Step Suck
   In this stroke, the air and fuel mixture is drawn into the cylinder. The intake valve opens when the valve is thrown away and closed. The piston moves downward, causing the cylinder to become a vacuum, and the entry of a mixture of air and fuel into the cylinder is caused by external air pressure (atmospheric pressure).
2. Step Compression
   In this stroke, the air-fuel mixture is compressed. The intake and exhaust valves were closed. As the piston begins to rise from the bottom dead center (BDC) to the top dead center (TDC), the inhaled mixture is compressed. Consequently, its pressure and temperature increase, making it more flammable. The crankshaft rotates once when the piston... reaches the TMA
3. Step Business During this stroke, the engine generates power to propel the vehicle forward. Just before the piston reaches the TDC during the compression stroke, the spark plug ignites the

compressed mixture. With the occurrence of burning, the strength from the pressure gas burning pushes the piston down. This effort produces the engine power.

4. Step Throw away In this stroke, the burned gases are expelled from the cylinders. The exhaust valve removes burned gases from the cylinder. The exhaust valve opens, and the piston moves from the BDC to the TDC, pushing the spent gases out of the cylinder. When the piston reaches the TDC, it moves again in preparation for the next stroke, which is the intake stroke. The crankshaft performs two full rotations in one cycle, consisting of four steps: suction, compression, power, and exhaust, which is the basis of how a 4-stroke engine works.

2.4 Cycle Ideal Motor Gas 4 Step

The thermodynamic and chemical processes occurring in gasoline engines are too complex to analyze theoretically (Neto et al., 2015). Therefore, this analysis requires imagining that these processes are in ideal conditions. Generally, the motor gas used cycle air as the ideal cycle (Ge et al., 2016). On cycle air volume constant (on cycle Otto) can depicted with chart pressure volume function, that is chart ρ–υ on Figure 4, which show diagram cycle Otto with income volume constant.

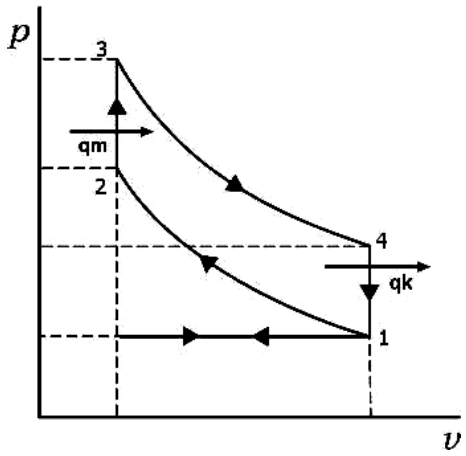

Figure 4. Diagram Cycle Otto

Where:

- q_m = amount heat Which entered
- q_k = amount of heat released

The ideal properties used and the description of the cycle process shown in Figure 4 are as follows:

- Curve 0–1 : Suction stroke at constant pressure.
- Curve 1–2 : Step compression, on-process isentropic.
- Curve 2–3 : Process burning on volume constant, process income heat on volume constant.
- Curve 3–4 : Work steps in the isentropic expansion process.
- Curve 4–1–0 : discard step.

2.5 Computational Fluid Dynamics (CFD)

Fluid flow, whether liquid or gas, is closely related to life. daily. For example, conditioning air for buildings and cars, burning in motor burn and propulsion systems, and the interaction of various objects with air or water, complex flows in heat exchangers, and chemical reactors are quite interesting to

research, investigate, and analyze. To meet these research needs, even at the design level, a tool is needed that can analyze or predict quickly and accurately. Thus, a science called computational fluid dynamics (CFD) was developed, also known in Indonesian as computational fluid flow dynamics (CFD).

2.6 Process Simulation CFD

In general, there are three stages that must be carried out when conducting a CFD simulation, namely Preprocessing, Matter This first in build and analyze CFD models. Technically is make make model in package CAD (computer aided design), make mesh the condition limit and properties of the fluid were then applied. Solvers (the core solution-finding program) calculated the conditions applied during preprocessing. Post-processing is the final step in the CFD analysis. This step organizes and interprets the CFD simulation data, which can take the form of images, curves, or animations.

2.7 Structure Program Fluent

Structure from component the can seen on Figure! 5

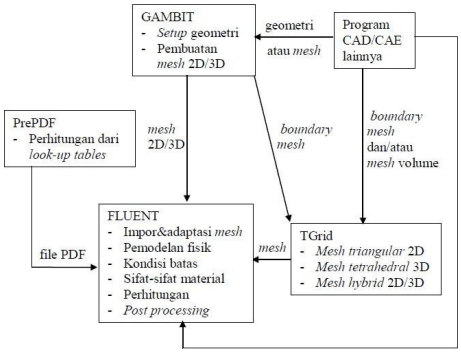

Figure 5. Structure Component Program Fluent
Source: (Tuakia, 2008)

Based on the Figure 5, the workflow outlines the process for setting up computational simulations. It starts with PrePDF for calculations and lookup tables, then moves to Gambit for geometry setup and mesh creation. The mesh is then imported and adapted into Fluent for physical modeling and computation. Alternatively, TGrid can be used for generating 2D or 3D meshes. The process ends with post-processing in Fluent, producing results in PDF format.

3. Methodology

Research methodology refers to the stages of research that must be established before problem-solving can be undertaken. This allows for focused research and facilitates the analysis of problems (Sunarya et al., 2018). The following flowchart of the research method used is shown in Figure 6.

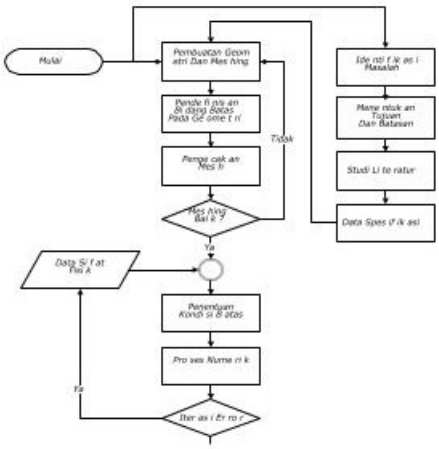

Figure 6. Research Flowchart

Based on Figure 6, the research process begins with data collection, followed by determining whether the data is suitable for analysis. If the data is suitable, the next step is the preparation and processing of the data. If not, the researcher will need to review and refine the data collection. After data processing, the next step involves conducting the analysis, followed by interpreting the results. Finally, the findings are used to draw conclusions and recommendations.

3.1 Procedure Retrieval Data

The data collection procedure, in the form of modeling, was performed using Autodesk Inventor software by creating a CAD model of the fluid domain to be simulated. The model was then exported into the iges format for compatibility with ANSYS FLUENT.

3.2 Specification Data And Calculation

- The air flow speeds were 10, 20, and 30 m/s.
- Temperature 300°K.
- Pressure 300000 Pa.
- Characteristics of the injector.

Characteristics injector based on injector brand: Accel, type: universal, with specification as following:

- Flow rate = 0.003 kg/s
- Vapor pressure = 3×10^5 bar
- Injection inner diameter = 0.0002 m
- Atomizer = 6

3.3 Modeling CAD Use Autodesk Inverter

This study examined the characteristics of gasoline injection in the intake manifold of a gasoline-powered internal combustion engine. The research was conducted using ANSYS FLUENT 17.1 software, a CFD program that uses the finite volume method (Afzal et al., 2017). Fluent provide flexibility mesh Which complete, so that can finish case flow Fluid modeling, even with an unstructured mesh (grid), is relatively easy (Gilmore et al., 2015; Gupta et al., 2020). The dimensions of this intake manifold model were based on the actual dimensions by directly measuring the geometry of the internal combustion engine in the thermal laboratory of the Energy Conversion Engineering Department, ISTN Jakarta. The internal

combustion engine is shown in Figure 7.

Figure 7. Photo Motor Gasoline In Lab. Thermal T. Conversion Energy ISTN
Source: Motor FORD 2271E, 1000 cc can operated with round 1000 rpm, 2000 rpm, 3000 rpm and 4000 rpm

Figure 8. Results Measurement Geometry Room Burn (Intake Manifold)

Based on Figure 7 and Figure 8, the steps for creating a CAD model in Autodesk Inventor are as follows: create a sketch based on the existing dimensions, perform a revolution to create a cylinder from the sketch, create a second inlet sketch at the center point of the cylinder, and extrude the inlet sketch to form a new cylinder.

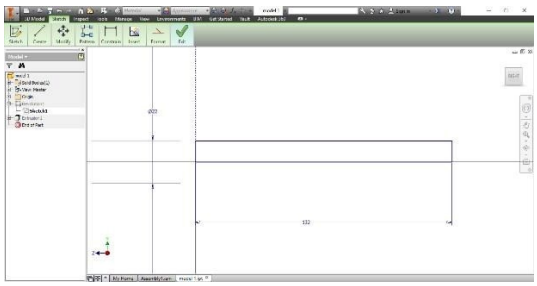

Figure 9. Design Sketch Geometry

Based on Figure 9, the following describes the steps taken in Autodesk Inventor software, designing Geometry Sketches, making sketches based on dimensions which are known, that is, in the form of picture piece cross-section of a half-cylinder, with a diameter guide line at the base of the box shape. This diameter guideline serves as the axis of rotation of the box sketch to form a cylinder.

3.4 Design Sketch Solid 3D

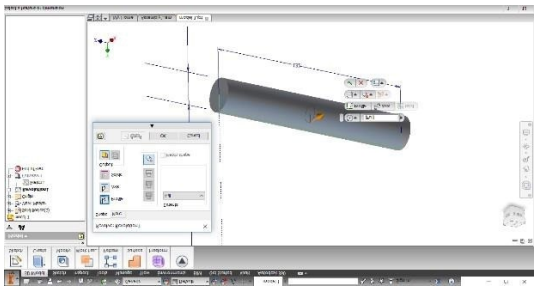

Figure 10. Design Sketch Solid 3D

Based on Figure 10, the sketch was revolved around the rotation axis, which is the base of the sketch, to create a 3D solid cylinder model. This step serves to "rotate" the box sketch we created around a specific rotation axis, which is the base of the box, along 360° or a full circle, to form a solid cylinder model.

3.5 Design Sketch Inlet road Outlet

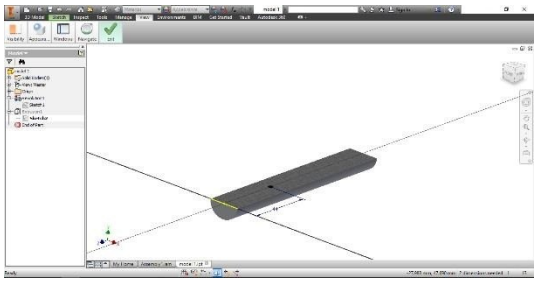

Figure 11. Design Sketch Diameter Inlet and Outle

Based on Figure 11, the inlet second was sketched with predetermined dimensions. The second is a circle that will later become the diameter of the outlet.

3.6 Design Extrude

The sketch is extruded to create a new cylinder. The circular sketch was extruded to create a solid cylinder model.

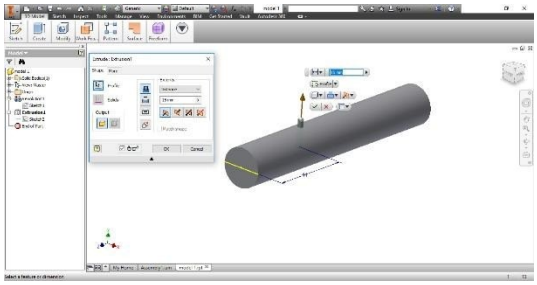

Figure 12. Design Sketch Diameter Inlet and Outlet

Based on Figure 12, from the existing geometric model and input data in the form of fuel properties and characteristics inputted as boundary conditions, researchers process the data into output in the form of flow patterns in the intake manifold using the ANSYS FLUENT program so that the data can be

analyzed and compared. Data retrieval in the form of flow patterns and characteristics was carried out in the ANSYS results, also known as post-processing.

3.7 Meshing and Input Boundary Condition Use ANSYS

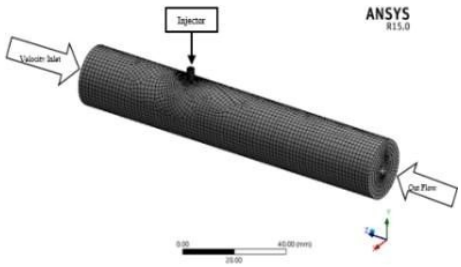

Figure 13. Modeling Intake Manifold

Based on Figure 13, this is a simulation model of a cylindrical object created in ANSYS, showing the mesh applied to the geometry. The injector is located at one end of the cylinder, and the flow of the material is analyzed within the cylindrical structure. The color scale at the bottom indicates the range of variable values (e.g., pressure or temperature) across the mesh, with the model likely being used for computational fluid dynamics (CFD) analysis.

3.8 Stages Simulation Numeric Use ANSYS

The following stages were simulated numerically using ANSYS:

1. Data specifications
   The speed flow air in the intake manifold was 10, 20, and 30 m/s. Temperature 300°K. Pressure 300 kPa.
2. Formulation Solver
   Select a solver formulation to produce accurate solutions for various types of cases using the Define → Models → Solver command. Then, the segregated unsteady solver formulation is selected for cases with incompressible and compressible fluids with low to medium fluid flow velocities (Mach number < 1).
3. Determine Equality Energy

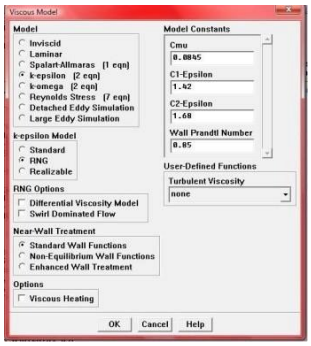

Figure 14. Viscous Model

Based pn Figure 14, the energy equations were activated the energy equations in FLUENT for simulations requiring the analysis of temperature, heat transfer, or radiation. These equations can be activated using the Define → Models → Energy command.

4. Determine Modeling Viscosity

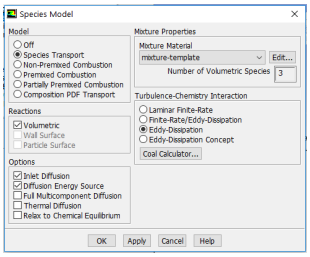

Figure 15. Species Model

Based on Figure 15, viscosity modeling was performed using the k-epsilon rng by executing the Define → Models → Viscous command. The k-epsilon model is a fairly complete turbulence model with two equations that allow the turbulent velocity and length scales to be determined independently.

5. Determine Model Species Transport And Reaction Chemistry

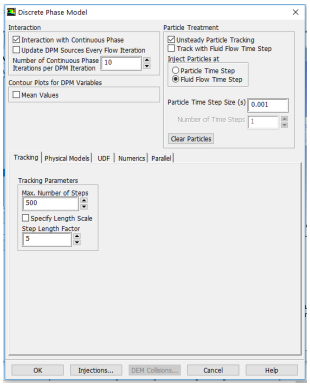

Figure 16. Discrete Phase Model

Based on Figure 16, species transport and chemical reaction models were defined using the Define → Models → Species → Transport → Species Transport command. Then, the volumetric reaction for the reaction occurring in the main phase is selected.

6. Determine Model Phase

The phase model was defined through the command Define → Models → Discrete Phase → Physical Models → Droplet Breakup → Tracking → Drag Parameter → Dynamic Drag. The discrete phase flow model was used for bubble and droplet flows, where the discrete phase volume was less than or equal to 10%.

7. Determine Type Injection (Injector)

Figure 17. The Accel Fuel Universal Injector

Based on Figure 18, the injection type was determined by executing the command Define → Injections → Create → Injection Type → Pressure Swirl Atomizer → Number of Particle Streams = 100 → Particle Type = Droplet → Material = Gasoline.

Product Enter the characteristics in the point properties as follows:

- Flow rate = 0.003 kg/s
- Vapor pressure = 3×10^5 injection bar
- Inner diameter = 0.0002 m
- Atomizer = 6

For sub-turbulent dispersion, the discrete random walk model was selected. The characteristics of the point properties above are based on the injector brand: Accel, type: universal, mass flow: 0.003 kg/s, pressure injection: 300000 Dad, Pressure = 3 bar, and injector orifice diameter: 0.2 mm = 0.0002 m.

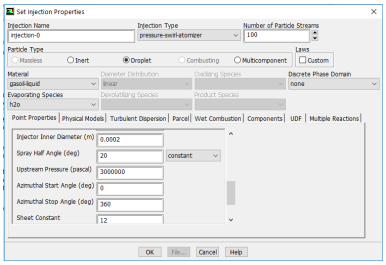

Figure 18. Set Injection Properties

8. Defining Characteristic Physique Material
   Define the physical properties of the material using the command Define → Materials → Material Type = Droplet Particle.
9. Determine Condition Limit And Parameter On Condition Limit
   The boundary conditions and parameters in the boundary conditions were defined using the command Define → Boundary Condition → Velocity Inlet → Velocity Magnitude = 10 m/s, 20 m/s, 30 m/s.
10. Determine Condition Limit Velocity Inlet
    The inlet velocity boundary conditions were used to define the flow rate and other switch quantities at the flow inlet.
11. Determine Parameter Control Solution

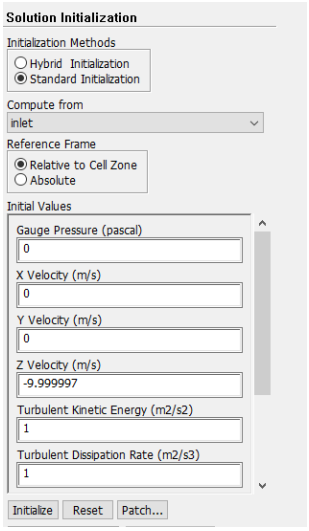

Figure 19. Solution Initialization

Based on Figure 19 determine the parameter control solution through the order Solve → Control → Solution.

12. Process Iteration

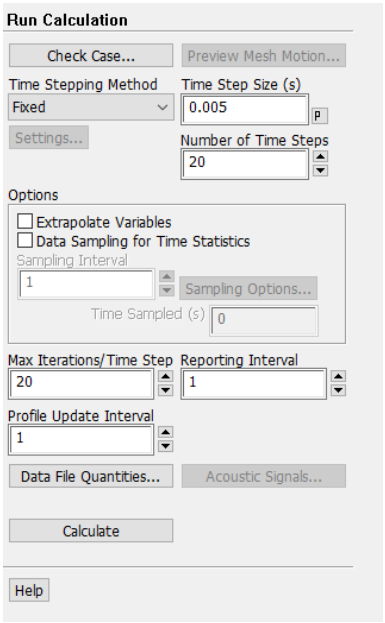

Figure 20. Run Calculation

Based on Figure 20, the iteration process requires initialization (an initial guess) before the calculation is started. This initialization process can be accessed via the command Solve → Initialize → Initialize → Compute From = All Zones → Initialize.

13. Do Calculation/Iteration

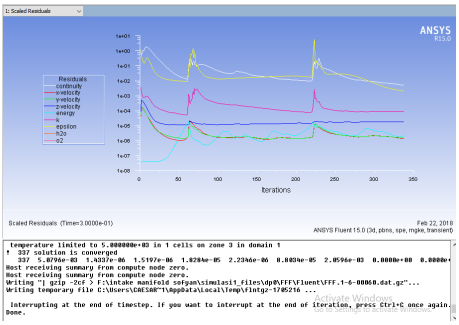

Figure 21. ANSYS Results Iteration

Based on Figure 21, the settings described above in ANSYS FLUENT, an iteration or calculation process was then carried out, namely, the process of finding solutions to the fluid flow equations in the domain we had previously created. To monitor whether the simulation converged, a residual plot was created so that when a divergent solution occurred, it could be immediately stopped and repeated with new settings. This is important considering that the time required for the iteration process can last up to several hours or even several days for complex simulations.

After the solution converged, the simulation data in Figure 21 were viewed in the ANSYS results graph for further processing. The following is a screenshot of the ANSYS results window when the data collection was performed.

Process manufacturing plot distribution of pressure.

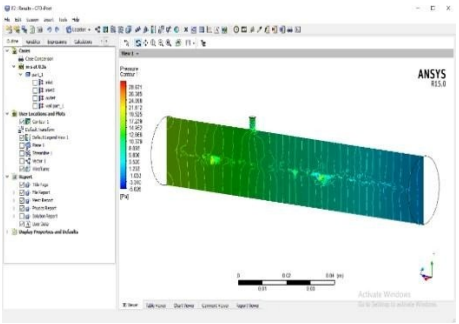

Figure 22. Plot Distribution Pressure

Figure 22 displays the pressure distribution within the system after the simulation converged. It shows how pressure varies across the geometry, providing insights into pressure gradients at different points within the structure.

Process of making velocity distribution plot

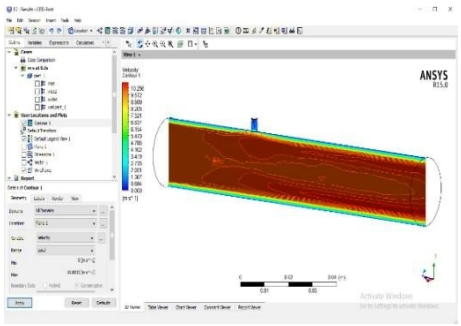

Figure 23. Plot Pattern Distribution Speed of Streamline

Figure23 illustrates the distribution of velocity throughout the system. The color-coded map helps to identify regions with high or low flow velocities, which is critical for understanding the fluid dynamics in the model.

Pattern Plot Making Process

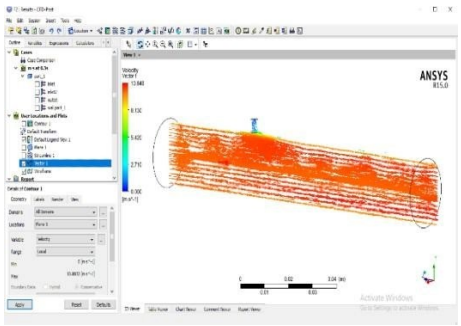

Figure 24. Plot Pattern Streamline

Figure 24 shows the streamline distribution, indicating the flow path of the fluid within the system. It provides a clear visualization of how the fluid moves through the geometry, allowing for an assessment of flow behavior and any potential flow separations or turbulence.

4. Results and Discussion

This study examined several variables representing the flow characteristics in the intake manifold with gasoline injection, including velocity and pressure contours, each of which varied according to the inlet velocities, namely 10 m/s, 20 m/s, and 30 m/s. This numerical study employed the ANSYS FLUENT software in a three-dimensional and transient simulation approach, where the changes over time were considered to represent actual conditions. To visualize the flow at the center region, the results were displayed on a 2D plane at $t = 0.1$ s. The flow direction occurred from left to right. The standard turbulence model used in ANSYS FLUENT was the RNG k-ε model because it is considered conservative for general fluid flow simulations and is known for its ease of convergence.

4.1 Analysis of Convergence

To determine whether the simulation was convergent or divergent, an indicator in the form of a residual plot was used. The residual plot consisted of several flow parameters, namely continuity, velocity in the x-direction, velocity in the y-direction, velocity in the z-direction, energy, k, ε, and the volume fraction of the fluid composition. The residual value indicates the accuracy of the simulation solution based on the

number of zeros after the decimal point. This implies that the smaller the residual value, the higher the likelihood that the simulation has converged. As shown in Figure 4.1, the residual plot generated from this simulation exhibits a decreasing trend in residual values, indicating that the simulation is converging.

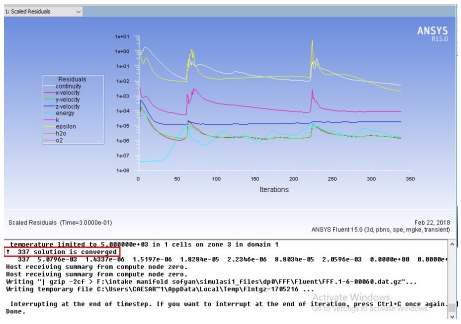

Figure 25. Ansys Result Convergence

Based on Figure 25, there are sudden fluctuations in the residual plot owing to the transient nature of the simulation or changes over time. In transient simulation, every few iterations, there is a change in the time step that requires the iteration to be repeated at the next time step. This repeated iteration at the beginning of the next time step is what causes the residual plot graph to appear to increase (it has nothing to do with the divergent solution). Then, to ensure that the solution was truly convergent, iterations were performed until a solution was obtained. reach criteria convergent each parameter flow. The solution reaches the convergence criteria when the warning " solution is converged " appears on the ANSYS FLUENT screen.

4.2 Distribution Contour Speed Flow Air

The following presents the velocity distribution contours of the airflow at various inlet velocities, namely 10 m/s, 20 m/s, and 30 m/s.

Velocity Distribution Contour of Airflow at Inlet Velocity 10 m/s

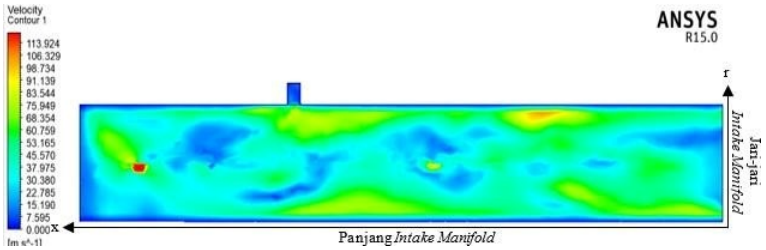

Figure 26. Distribution Contour Speed Flow Air On Speed Inlet 10 m/s

Distribution of air flow velocity contours at an inlet velocity of 20 m/s

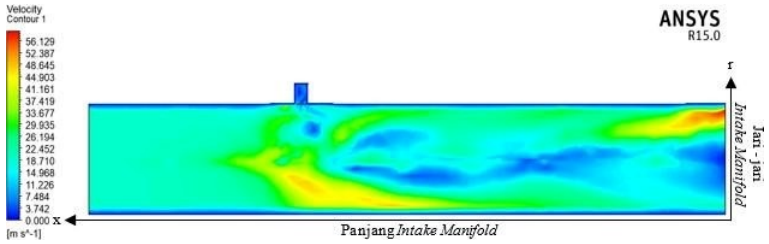

Figure 27. Distribution Contour Speed Flow Air On Speed Inlet 20 m/s

Distribution of air flow velocity contours at inlet velocity 30 m/s

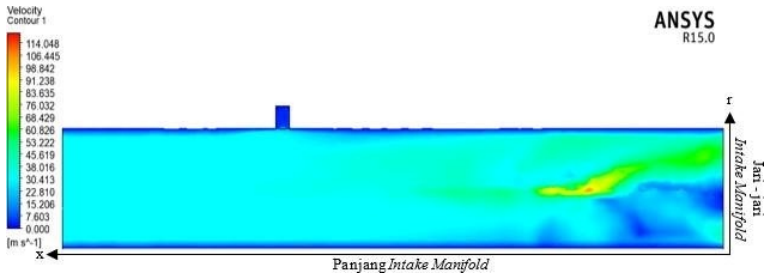

Figure 28. Distribution Contour Speed Flow Air On Speed Inlet 20 m/s

Figure 26, Figure 27, and Figure 28 shows that the velocity distribution contains points with relatively high velocities, as indicated by the central red contour. These points with the highest velocities indicated the location of the particles injected into the intake manifold. The image shows the event at 0.1s. The greater the inlet velocity, the farther the injection particles traveled from the inlet position. It can also be seen from the velocity contour pattern above that the velocity distribution pattern is also more even at the inlet velocity. low, indicating that the fuel distribution in the intake manifold was more uniform at the inlet speed low. The area near the wall was blue, indicating a low velocity. This is due to the boundary layer effect. This low velocity indicates an area with poor mixing of gasoline and air.

4.3 Distribution Vector Speed

To support the information presented by the velocity contour pattern, the velocity vector distribution is also presented so that the flow pattern can be seen more clearly, along with the direction of the velocity vector. The following shows the velocity vector distributions at various inlet velocities. namely 10 m/s, 20 m/s and 30 m/s.

The distribution vector speed on the speed inlet was 10 m/s

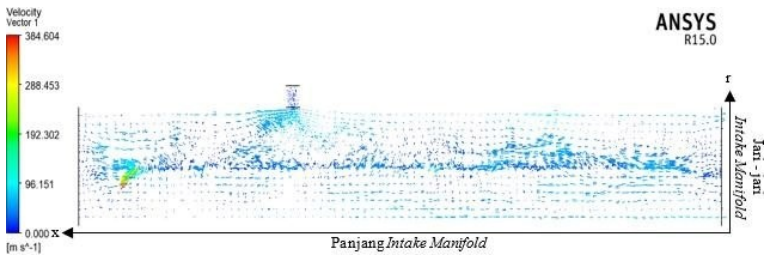

Figure 29. Distribution Vector Speed On Speed Inlet 10 m/s

Distribution of velocity vector at inlet velocity 20 m/s

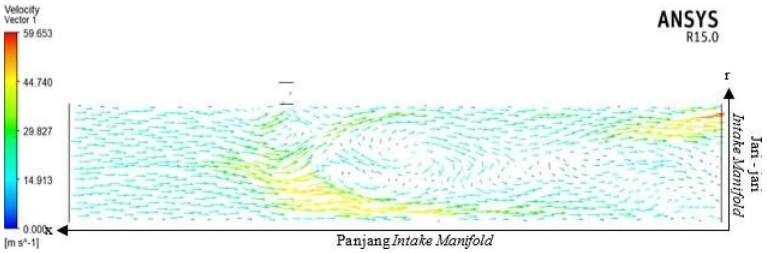

Figure 30. Distribution Vector Speed On Speed Inlet 20 m/s

Distribution of the velocity vector at the inlet velocity of 30 m/s

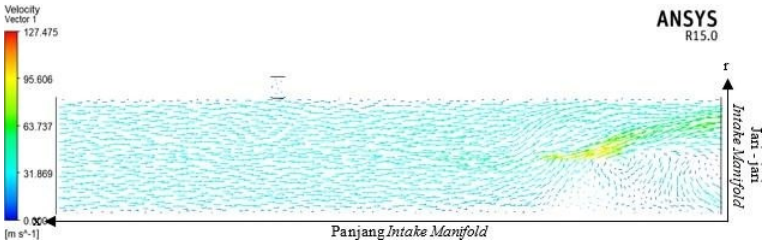

Figure 31. Distribution Vector Speed On Speed Inlet 30 m/s

Based on Figure 29, Figure 30, and Figure 31, it can be observed that there are points with very high velocities marked in red, whose positions are identical to those shown in the velocity contour distribution. Use visualization vector This, We can see pattern flow Which happen on surroundings point The injection particles, or areas in red, experience a vortex centered toward the particle spray area. This indicates the mixing of air and gasoline particles at that location. The streamlined pattern exhibited a rolling flow in the fuel injection area. This is advantageous in terms of the fuel-air mixing quality, but it creates pressure. drop or decrease in pressure, such that some of the kinetic energy is lost. Possible solutions to this problem are that the swirler uses a more localized method to mix fuel with air, so that the pressure drop does not occur over a large area.

4.4 Distribution Contour Pressure

One of the important parameters to consider in fluid flow analysis is the distribution of pressure patterns and contours in the flow. The following shows the distribution of the velocity vectors at various inlet velocities namely 10 m/s, 20 m/s and 30 m/s.

The distribution contour pressure on the speed inlet was 10 m/s.

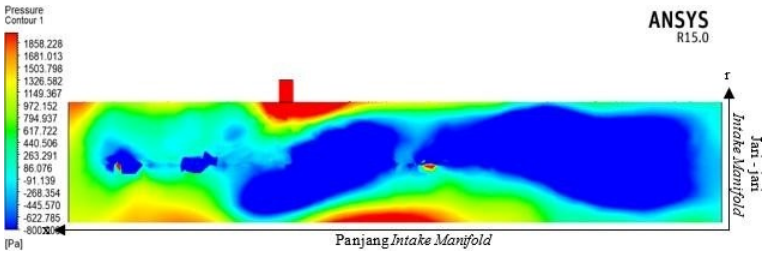

Figure 32. Distribution Contour Pressure On Speed Inlet 10 m/s

Pressure contour distribution at inlet velocity 20 m/s.

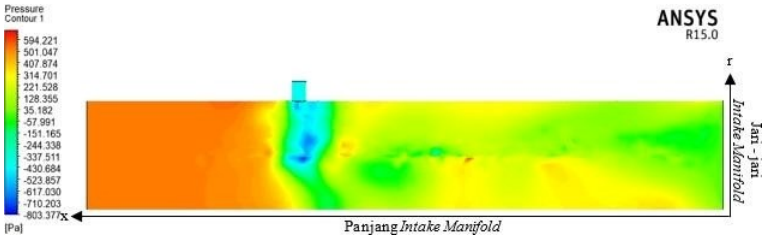

Figure 33. Distribution Contour Pressure On Speed Inlet 20 m/s

The distribution contour pressure on the speed inlet was 30 m/s.

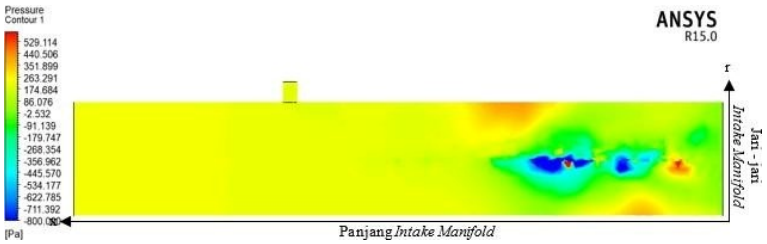

Figure 34. Distribution Contour Pressure On Speed Inlet 30 m/s

Based on Figure 32, Figure 33, and Figure 34, the inlet area has a higher pressure than the outlet area. This occurs because of the pressure drop in the system caused by friction with the intake manifold walls or the rolling flow pattern, which reduces the kinetic energy. The high-velocity region observed from the velocity contour and velocity vector above in this pressure contour can be observed to be blue, or in other words, it becomes very low or even negative. This occurs according to Bernoulli's law: the higher the velocity, the higher the pressure. location the will the more low. As for pressure Which low the result in suction fluid into it, which can be observed in the velocity vector pattern that tends towards the direction of the particle spray. The trend in the pressure contour is identical to that of the velocity contour, namely, the center of the minimum pressure increasingly shifts to the left or shifts more quickly and becomes more evenly distributed with increasing inlet velocity. The pressure contour shows a decrease in pressure from the inlet. to the outlet, which strengthens the explanation of the vector plot, so that the solution provided is identical to the previous explanation.

5. Conclusions

From the numerical analysis that produced data in the form of contour and vector plots at various inlet velocity variations, varying output results were obtained. The settings in ANSYS FLUENT indicated the occurrence of areas with high speed or low pressure at certain points, namely the points where the spray occurred. It can be observed from the velocity distribution pattern that the point areas with high velocities tended to shift more rapidly as the inlet velocity increased. From the velocity distribution pattern, it can also be seen that the wall region has low velocities owing to the boundary layer effect. This low velocity indicated poor fuel-air mixing. Furthermore, the velocity vector distribution pattern supports the explanations above by showing the flow direction. A vortex pattern occurred around the spray point, indicating the mixing of fuel and air. The pressure distribution pattern indicates the same trend as the velocity distribution pattern, namely a relatively faster shift at higher inlet velocity inputs. The spray point in the pressure distribution pattern is indicated by the low-pressure area (blue), considering that Bernoulli's law states that the higher the speed, the lower the pressure.

Acknowledgements

Author would like to express our gratitude to the the Department of Energy Conversion Engineering at the ISTN Jakarta, Indonesia for providing the resources and laboratory space for this research. Special thanks go to the technical staff for their assistance with the equipment and software tools. Author also appreciate the valuable feedback from our colleagues and mentors who guided us throughout the study.

Author Contributions

RHS conceptualized the study, designed the methodology, conducted the literature review, collected the data, and provided final approval for the manuscript.

Conflicts of Interest

The authors declare that there is no conflict of interest regarding the publication of this study. This research was conducted independently, and no financial or personal relationships influenced the results or interpretation of the findings.

References

Abdullah, M. A. F. (2021). Analysis of consumer motives in purchasing decisions and the use of instant cooking seasonings. *Jurnal Bisnis, Ekonomi, Manajemen, Dan Kewirausahaan*, *1*(1), 27–35. https://doi.org/10.52909/jbemk.v1i1.24

Abu-Qudais, M. D., Asfar, K. R., & Al-Azzam, R. (2001). Engine performance using vaporizing carburetor. *Energy Conversion and Management*, *42*(6), 755–761. https://doi.org/10.1016/S0196-8904(00)00098-4

Afzal, A., Ansari, Z., Faizabadi, A. R., & Ramis, M. K. (2017). Parallelization strategies for computational fluid dynamics software: State of the art review. *Archives of Computational Methods in Engineering*, *24*(2), 337–363. https://doi.org/10.1007/s11831-016-9165-4

Agusinta, L., Nugroho, A. E., Fachrial, P., & Suryawan, R. F. (2021). Assessment model of employee competence, ground support equipment effectiveness, and satisfaction on service quality. *Jurnal Transportasi, Logistik, dan Aviasi*, *1*(1), 55–69. https://doi.org/10.52909/jtla.v1i1.37

Aljaberi, H. A., Aziz, N. A., & Hairuddin, A. A. (2018). Cfd modeling and experimental validation of different piston crown designs in an hcci engine fuelled with iso-octane. *Journal of Engineering and Applied Sciences*, *13*(12), 4286–4299.

Aljaberi, H. A., Hairuddin, A. A., & Aziz, N. A. (2017). The use of different types of piston in an hcci engine: A review. *International Journal of Automotive and Mechanical Engineering*, *14*(2), 4348–4268. https://doi.org/10.15282/ijame.14.2.2017.17.0346

Anakottapary, D. S. (2020). Fuel consumption analysis of injection system and carburetor system on honda beat fi 2013. *Logic: Jurnal Rancang Bangun dan Teknologi*.

Andwari, A. M., Muhamad Said, M. F., Abdul Aziz, A., Esfahanian, V., Zadeh, A. S., Idris, M. A., & Jamil, H. M. (2018). Design, modeling and simulation of a high-pressure gasoline direct injection (gdi) pump for small engine applications. *Journal of Mechanical Engineering (JMechE)*, (1), 107–120. https://doi.org/10.56381/jsaem.v2i1.72

Anggraini, D. (2021). The impact of covid-19 on stock price changes. *Jurnal Bisnis, Ekonomi, Manajemen, Dan Kewirausahaan*, *1*(1), 1–18. https://doi.org/10.52909/jbemk.v1i1.22

Aprillita, D., & Perkasa, D. H. (2021). The impact of the covid-19 pandemic on consumer purchasing power in the online retail sectors. *Jurnal Bisnis, Ekonomi, Manajemen, Dan Kewirausahaan*, *1*(1), 19–26. https://doi.org/10.52909/jbemk.v1i1.23

Ayuningtyas, B., & Ilman, S. (2021). Ip camera surveillance system using an android application based on arduino. *Jurnal Teknika Dan Informatika*, *1*(1), 1–18. https://doi.org/10.52909/jti.v1i1.6

Barot, M., Shah, A., & Patel, M. (2017). Cfd analysis of single cylinder four stroke gas fueled engine for prediction of air flow rate during suction stroke. *International Journal of Engineering Development and Research*, *5*(2), 1135–1140.

Benajes, J., García, A., Monsalve-Serrano, J., & Boronat, V. (2017). Achieving clean and efficient engine operation up to full load by combining optimized rcci and dual-fuel diesel-gasoline combustion strategies. *Energy Conversion and Management*, *136*, 142–151. https://doi.org/10.1016/j.enconman.2017.01.010

Berlian Rms, A., & Wahyuningsih, E. (2021). Analysis of frictional energy generation between train wheels and rails. *Jurnal Teknika Dan Informatika*, *1*(1), 46–61. https://doi.org/10.52909/jti.v1i1.10

Chala, G. T., Abd Aziz, A. R., & Hagos, F. Y. (2018). Natural gas engine technologies: Challenges and energy sustainability issue. *Energies*, *11*(11), 2934. https://doi.org/10.3390/en11112934

Descombes, G., Maroteaux, F., & Feidt, M. (2003). Study of the interaction between mechanical energy and heat exchanges applied to ic engines. *Applied Thermal Engineering*, *23*(16), 2061–2078. https://doi.org/10.1016/S1359-4311(03)00160-1

Dinh, T., Nguyen, K., Pham, T., & Nguyen, V. (2020). Study on performance enhancement and emission reduction of used carburetor motorcycles fueled by flex-fuel gasoline-ethanol blends. *Journal of the Chinese Institute of Engineers*, *43*(5), 477–488. https://doi.org/10.1080/02533839.2020.1751719

Galamboš, S. L., Nikolić, N. M., Ružić, D. A., & Dorić, J. Ž. (2020). An approach to computational fluid dynamic air-flow simulation in the internal combustion engine intake manifold. *Thermal Science*, *24*(1 Part A), 127–136. https://doi.org/10.2298/tsci180707063g

Ge, Y., Chen, L., & Sun, F. (2016). Progress in finite time thermodynamic studies for internal combustion engine cycles. *Entropy*, *18*(4), 139. https://doi.org/10.3390/e18040139

Gilmore, R. C., Marts, J. A., Brune, J. F., Saki, S., Bogin Jr, G. E., & Grubb, J. W. (2015). Simplifying cfd modeling. *Mining Engineering*, *67*(3), 68–72.

Goyal, H., Kook, S., & Ikeda, Y. (2019). The influence of fuel ignition quality and first injection proportion on gasoline compression ignition (gci) combustion in a small-bore engine. *Fuel*, *235*, 1207–1215. https://doi.org/10.1016/j.fuel.2018.08.090

Gupta, N., Bhardwaj, N., Khan, G. M., & Dave, V. (2020). Global trends of computational fluid dynamics to resolve real world problems in the contemporary era. *Current Biochemical Engineering*, *6*(3), 136–155. https://doi.org/10.2174/2212711906999200601121232

Heriyanto, D. (2021). The impact of service quality and compensation on crew satisfaction in manning companies. *Jurnal Transportasi, Logistik, dan Aviasi*, *1*(1), 31–41. https://doi.org/10.52909/jtla.v1i1.35

Holkar, R., Sule-Patil, Y. N., Pise, S. M., Godase, Y. A., & Jagadale, V. S. (2015). Numerical simulation of steady flow through engine intake system using cfd. *IOSR Journal of Mechanical and Civil Engineering (IOSR-JMCE)*, *12*(1), 30–45. https://doi.org/10.9790/1684-12123045

Ikeya, K., Takazawa, M., Yamada, T., Park, S., & Tagishi, R. (2015). Thermal efficiency enhancement of a gasoline engine. *SAE International Journal of Engines*, *8*(2015-01-1263), 1579–1586. https://doi.org/10.4271/2015-01-1263

Inam, S. A., Hussain, M., & Baig, M. M. (2019). Numerical simulation of liquid fuel injection in combustion chamber. *Arabian Journal for Science and Engineering*, *44*(6), 5889–5895. https://doi.org/10.1007/s13369-019-03774-1

Jumadi, R., Khalid, A., Jaat, N., Abdullah, I. S., Darlis, N., Manshoor, B., & Nursal, R. S. (2020). Analysis of spray characteristics and high ambient pressure in gasoline direct injection using computational fluid dynamics. *CFD Letters*, *12*(5), 36–51. https://doi.org/10.37934/cfdl.12.5.3651

Kalghatgi, G., & Johansson, B. (2018). Gasoline compression ignition approach to efficient, clean and affordable future engines. *Proceedings of the Institution of Mechanical Engineers, Part D: Journal of Automobile Engineering*, *232*(1), 118–138. https://doi.org/10.1177/0954407017694275

Kalita, P., & Titabor, J. (2016). Alternative fuel for ic engine: Review the effect from ethanol in carburetor. *International Journal of Computer Engineering in Research Trends*, *3*(7), 371–376. https://doi.org/05.2016-75251336/IJCERT.2016.3701

Keke, Y., Tobing, N. G. L., & Tanjung, I. (2021). The effect of occupational safety and health on employee performance at pt. angkasa kargo. *Jurnal Transportasi, Logistik, dan Aviasi*, *1*(1), 42–54. https://doi.org/10.52909/jtla.v1i1.36

Kuncoro, H., & Harahap, V. (2021). Effect of electronic flight bag usage and safety culture on flight safety performance at pt. garuda indonesia. *Jurnal Transportasi, Logistik, dan Aviasi*, *1*(1), 18–30. https://doi.org/10.52909/jtla.v1i1.34

Kunze, J., & Stimming, U. (2009). Electrochemical versus heat-engine energy technology: A tribute to wilhelm ostwald's visionary statements. *Angewandte Chemie International Edition*, *48*(49), 9230–9237. https://doi.org/10.1002/anie.200903603

Mishra, P. C., Kar, S. K., Mishra, H., & Gupta, A. (2016). Modeling for combined effect of muffler geometry modification and blended fuel use on exhaust performance of a four stroke engine: A computational fluid dynamics approach. *Applied Thermal Engineering*, *108*, 1105–1118. https://doi.org/10.1016/j.applthermaleng.2016.08.009

Nassiri, T. A., Kakaee, A. H., & Ebne-Abbasi, H. (2017). Exhaust gas heat recovery through secondary expansion cylinder and water injection in an internal combustion engine. *Thermal Science*, *21*(1 Part B), 729–743. https://doi.org/10.2298/TSCI150915282N

Neto, A. F. G., Lopes, F. S., Carvalho, E. V., Huda, M. N., Neto, A. M. J. C., & Machado, N. T. (2015). Thermodynamic analysis of fuels in gas phase: Ethanol, gasoline and ethanol-gasoline predicted by dft method. *Journal of Molecular Modeling*, *21*(10), 267. https://doi.org/10.1007/s00894-015-2815-x

Parmenas, N. H. (2021). Strategies for maintaining employee well-being during the covid-19 pandemic. *Journal of Economics, Management, Entrepreneurship, & Business*, *1*(1), 15–31. https://doi.org/10.52909/jemeb.v1i1.3

Rao, K. V. S., Kurbet, S. N., & Kuppast, V. V. (2018). A review on performance of the ic engine using alternative fuels. *Materials Today: Proceedings*, *5*(1), 1989–1996. https://doi.org/10.1016/j.matpr.2017.11.303

Ricardianto, P., Sakti, R. F. J., Sembiring, H. F. A., & Abidin, Z. (2021). Safety performance analysis of state and commercial ships in accordance with solas 1974. *Journal of Economics, Management, Entrepreneurship, & Business*, *1*(1), 1–14. https://doi.org/10.52909/jemeb.v1i1.2

Saputro, A., & Soleha, I. (2021). Analysis of the performance of extraction-condensing turbine unit 1 at bablean power plant. *Jurnal Teknika Dan Informatika*, *1*(1), 62–79. https://doi.org/10.52909/jti.v1i1.11

Satria, B. (2021). The effect of transformational leadership and work motivation on employee performance at pt. xyz. *Jurnal Bisnis, Ekonomi, Manajemen, Dan Kewirausahaan*, *1*(1), 36–47. https://doi.org/10.52909/jbemk.v1i1.25

Setyawati, A., & Aristiyanto, F. K. (2021). Improving discipline through apron movement control (amc) at pt angkasa pura i adi soemarmo airport. *Jurnal Transportasi, Logistik, dan Aviasi*, *1*(1), 1–17. https://doi.org/10.52909/jtla.v1i1.33

Setyawati, A., Huda, M. N., Suripno, S., & Tannady, H. (2021). Analysis of integrated bus terminal services and their impact on customer satisfaction at pulo gebang. *Journal of Economics, Management, Entrepreneurship, & Business*, *1*(1), 44–55. https://doi.org/10.52909/jemeb.v1i1.5

Solihin, A. (2021). The effect of workload, compensation, and career development on employee loyalty at pt. abc. *Jurnal Bisnis, Ekonomi, Manajemen, Dan Kewirausahaan*, *1*(1), 48–58. https://doi.org/10.52909/jbemk.v1i1.26

Sunarya, P. A., Budiarto, E., & Lestari, F. H. N. (2018). Improved management understanding of research through concepts and preliminary studies for empirical problem solving. *APTISI Transactions on Management*, *2*(2), 89–96.

Susanto, P. C., & Parmenas, N. H. (2021). Development of a succession planning model for insurance subsidiaries. *Journal of Economics, Management, Entrepreneurship, & Business*, *1*(1), 56–75. https://doi.org/10.52909/jemeb.v1i1.16

Susanto, P. C., Suryawan, R. F., Hartono, H., & Purwoko, B. A. (2021). Analysis of accident-prone areas along the ciawi–puncak road, bogor. *Journal of Economics, Management, Entrepreneurship, & Business*, *1*(1), 32–43. https://doi.org/10.52909/jemeb.v1i1.4

Syahrial, E., & Sudono, R. H. (2021). Cooling load analysis of a new building at pmi bogor hospital using the cltd method. *Jurnal Teknika Dan Informatika*, *1*(1), 34–45. https://doi.org/10.52909/jti.v1i1.9

Tuakia, F. (2008). *Dasar-dasar cfd menggunakan fluent*. Penerbit Informatika.

Wahyuningsih, E., Widodo, S., & Rahmanto, R. (2021). Prototype manufacture of the arjuno autobost covid-19 robot. *Jurnal Teknika Dan Informatika*, *1*(1), 19–33. https://doi.org/10.52909/jti.v1i1.8

Wallington, T. J., Kaiser, E. W., & Farrell, J. T. (2006). Automotive fuels and internal combustion engines: A chemical perspective. *Chemical Society Reviews*, *35*(4), 335–347. https://doi.org/10.1039/B410469M

Xu, C. C., & Choa, H. M. (2016). The analysis of the cfd about the swirl generation in four-stroke engine. *International Journal of Applied Engineering Research*, *11*(16), 8940–8945. https://doi.org/10.4172/2168-9873.1000221